Journal of Microbiology, Immunology and Infection 57 (2024) 647—659

Available online at www.sciencedirect.com

ScienceDirect

journal homepage: www.e-jmii.com

Original Article

Curative effects and mechanisms of AG1296 and LY294002 co-therapy in *Angiostrongylus cantonensis*-induced neurovascular unit dysfunction and eosinophilic meningoencephalitis

Ke-Min Chen [a], **Shih-Chan Lai** [a,b,*]

[a] *Department of Parasitology, Chung Shan Medical University, Taichung 402, Taiwan*
[b] *Clinical Laboratory, Chung Shan Medical University Hospital, Taichung 402, Taiwan*

Received 10 April 2023; received in revised form 6 May 2024; accepted 28 May 2024
Available online 30 May 2024

KEYWORDS
Angiostrongylus cantonensis;
Meningoencephalitis;
MMP-9;
PDGFR-β;
Signaling pathway

Abstract *Background:* Co-therapy with albendazole and steroid is commonly used in patients with eosinophilic meningoencephalitis caused by *Angiostrongylus cantonensis* infections. However, anthelminthics often worsen symptoms, possibly due to the inflammatory reaction to antigens released by dying worms. Therefore, the present study was to investigate the curative effects and probable mechanisms of the platelet-derived growth factor receptor-beta (PDGFR-β) inhibitor AG1296 (AG) and the phosphoinositide 3-kinase inhibitor (PI3K) LY294002 (LY) in *A. cantonensis*-induced neurovascular unit dysfunction and eosinophilic meningoencephalitis.
Methods: Western blots were used to detect matrix protein degradation and the expressions of PDGFR-β/PI3K signaling pathway. The co-localization of PDGFR-β and vascular smooth muscle cells (VSMCs), and metalloproteinase-9 (MMP-9) and VSMCs on the blood vessels were measured by confocal laser scanning immunofluorescence microscopy. Sandwich enzyme-linked immunosorbent assays were used to test S100B, interleukin (IL)-6, and transforming growth factor beta in the cerebrospinal fluid to determine their possible roles in mouse resistance to *A. cantonensis*.
Results: The results showed that AG and LY cotherapy decreased the MMP-9 activity and inflammatory reaction. Furthermore, S100B, IL-6 and eosinophil counts were reduced by inhibitor treatment. The localization of PDGFR-β and MMP-9 was observed in VSMCs. Furthermore, we showed that the degradation of the neurovascular matrix and blood-brain barrier permeability were reduced in the mouse brain.
Conclusions: These findings demonstrate the potential of PDGFR-β inhibitor AG and PI3K inhibitor LY co-therapy as anti-*A. cantonensis* drug candidates through improved neurovascular unit dysfunction and reduced inflammatory response.

* Corresponding author. Department of Parasitology, Chung Shan Medical University, Taichung 402, Taiwan.
E-mail address: shih@csmu.edu.tw (S.-C. Lai).

https://doi.org/10.1016/j.jmii.2024.05.012

Introduction

The rat lungworm *Angiostrongylus cantonensis* is a parasitic nematode that causes severe central nervous system (CNS) dysfunction and induces eosinophilic meningitis or meningoencephalitis.[1,2] Matrix metalloproteinase-9 (MMP-9) is an important proteolytic enzyme that can contribute to blood-brain barrier (BBB) in angiostrongyliasis meningoencephalitis.[3] The BBB is considered a part of the neurovascular unit, a concept that emphasizes the importance of cell—cell signaling between all cell types residing in neuronal, glial, and vascular compartments.[4] The interactions between these cellular components and inter- and intra-cellular signaling regulate neurovascular unit function to maintain homeostasis or to respond to inflammation and diseases.[5] The migration of vascular smooth muscle cells (VSMCs) requires the proteolytic degradation or remodeling of the matrix. MMPs catalyze and remove the basement membrane around VSMCs and facilitate their contact with the interstitial matrix.[6] For understanding of curative effects of AG1296 and LY294002 co-therapy in *A. cantonensis*-induced neurovascular unit dysfunction, we would focus on the integrity of the neurovascular matrix in treatment and diseased states.

Platelet-derived growth factor (PDGF), which is released by platelets, endothelial cells, and numerous other cells at the site of injury, is the most potent VSMC mitogen.[7] Binding of PDGF to the PDGF receptor (PDGFR) activates various downstream signaling proteins; mitogen-activated protein kinase signaling plays an important role in the regulation of proliferation, migration, and survival of mammalian cells.[8] Abnormalities in this signaling pathway are implicated in neurological diseases, especially in neurovascular dysfunction; neuroinflammation plays a prominent role in disease pathologies.[9] The phosphoinositide 3-kinase/protein kinase B (PI3K/Akt) signaling pathways enhance MMP expression and activity.[10] The activation of the PI3K/Akt signaling pathway is probably required for the production of MMP-9 in VSMCs in neurovascular unit. Therefore, we investigate the curative mechanisms of AG1296 and LY294002 co-therapy in *A. cantonensis*-induced neurovascular unit dysfunction and eosinophilic meningoencephalitis.

BBB leakage in CNS disorders can be thought of as a manifestation of neurovascular unit dysfunction.[11] We found neurovascular unit dysfunction in mice with eosinophilic meningoencephalitis after *A. cantonensis* infection. Co-therapy with albendazole and steroid is commonly used in patients with eosinophilic meningoencephalitis caused by infections of *A. cantonensis*. However, anthelminthics often worsen symptoms, possibly due to the inflammatory reaction to antigens released by dying worms. Thus, the present study was to evaluate the curative effects and probable mechanisms of AG and LY co-therapy in *A. cantonensis*-induced neurovascular unit dysfunction and eosinophilic meningoencephalitis.

Materials and methods

Experimental animals

Wild-type C57BL/6 male mice were purchased from the National Laboratory Animal Center (Taipei, Taiwan). MMP-9 knockout mice (B6.FVB (Cg)-*Mmp9*^{tm1Tvu}/J) were purchased from Jackson Laboratory (Bar Harbor, ME, US), and all intron 2 and a part of exon 2 were replaced with a cassette that contained the neomycin phosphotransferase gene, which was driven by the phosphoglycerate kinase promoter for MMP-9 knockout mice. All feeds, water, beddings, and cages for MMP-9 knockout mice were sterilized before use. All mice were kept in a temperature controlled environment at a 12 h light/dark cycle photoperiod and provided with Purina Laboratory Chow and water *ad libitum*. Five-week-old MMP-9 knockout and wild-type mice were kept in individual ventilated caging systems in a pathogen-free animal room (Chung-Shan Medical University, Taichung, Taiwan) for more than one week prior to experimental infection. After *A. cantonensis* infection, mice were monitored for signs of illness (decreased activity, ruffled fur, or tachypnea) and weight loss. No mortality was observed in the mice during their infection and drug treatment. The mice were maintained under CO_2 flow for at least 1 min after respiratory arrest. Cervical dislocation was performed as a confirmatory euthanasia prior to necropsy. All procedures and experiments were approved by the Institutional Animal Care and Use Committee of Chung-Shan Medical University and according to the institutional guidelines for animal experiments. The data obtained met the appropriate ethical requirements.

Antibodies

The goat anti-mouse phosphorylated polyclonal antibody PI3K (p-PI3K), the goat anti-mouse phosphorylated Akt (p-Akt) polyclonal antibody, the goat anti-mouse collagen type IV polyclonal antibody and goat anti-mouse fibronectin polyclonal antibody were purchased from Santa Cruz Biotechnology (CA, USA). Goat anti-mouse p-PDGFR-β polyclonal antibody was purchased from Cell Signaling Technology (Danvers, MA, USA). Mouse smooth muscle alpha (SM-α)-actin monoclonal antibody was obtained from Sigma (St. Louis, MO, USA). The goat anti-mouse MMP-9 polyclonal antibody was purchased from R&D Systems (Minneapolis, MN, USA). Mouse anti-mouse β-actin monoclonal antibody was acquired from Sigma (St. Louis, MO, USA).

Larval preparation

Infectious larvae (third stage, L3) of *A. cantonensis* were obtained from *Achatina fulica* snails, which were propagated for several months and infected with larvae of the first stage

of *A. cantonensis* by rats at the Wufeng Experimental Farm (Taichung, Taiwan). The L3 larvae within the tissues were recovered using a previously described method but with several modifications.[12] The snail shells were crushed, and the tissues were homogenized in a pepsin-HCl solution (pH 1—2, 500 IU pepsin/g tissue) and digested by agitation at 37 °C for 2 h. The L3 larvae in the sediment were collected by serial washes with double-distilled water and counted under a microscope. The identity of the L3 larvae of *A. cantonensis* was confirmed as previously described.[13]

Animal infection

A total of 20 MMP-9 knockout male mice were randomly assigned to uninfected control group and the infected group. Uninfected control mice were orally administered with distilled water only on day 10 after inoculation (PI). The infected group was infected with 30 *A. cantonensis* L3 larvae by oral inoculation and sacrificed on days 20 PI. Brains and CSF were collected for biochemical analysis and histopathological study, respectively.

Treatment of animals

A total of 100C57BL/6 wild-type mice were randomly divided into five groups (20 mice/group). Water and food were held for 12 h before infection. Uninfected control mice were orally administered with distilled water only on day 10 after inoculation (PI). All other groups were infected with 30 *A. cantonensis* L3 larvae, including infected control mice that were orally treated with distilled water only on day 10 PI. The treatment mice were treated separately with AG1296 (AG) alone (10 mg/kg/day, Cayman Chemicals, Ann Arbor, MI, USA), LY294002 (LY) (25 mg/kg/day, Sigma, St. Louis, MO, USA), and AG—LY co-treatment for 7 consecutive days starting on day 10 PI. The mice were sacrificed at 20 days PI. A group of 20 mice were selected for further tests, namely, 5 for biochemical analysis (zymography and Western blotting), 5 for Evans Blue analysis, 5 for enzyme-linked immunosorbent assay (ELISA) analysis, and 5 for histology.

Cerebrospinal fluid (CSF) collection

A single CSF sample was collected from the cisterna magna for ELISA and zymography assays. The mice were anesthetized by intraperitoneal urethane (1.25 g/kg) injection. Each mouse was placed in a stationary instrument at 135° from the head and body. The neck skin was shaved and swabbed thrice with 70% ethanol. The subcutaneous tissue and muscles were separated. A capillary tube was inserted through the dura mater into the citerna magna, and CSF was poured into the capillary tube as previously described.[3] The CSF was injected into a 0.5 mL Eppendorf tube and centrifuged at 3000×*g* at 4 °C for 5 min. The supernatant was collected in a 0.5 mL Eppendorf tube and kept in a freezer at −80 °C.

Western blot analysis

Electrophoresis and the following Western blot analysis are indispensable to investigate protein changes in brain tissues. Brain tissue homogenates were centrifuged at 10,000×*g* at 4 °C for 10 min to remove the debris. Proteins (30 μg) of the supernatant were determined using protein assay kits (Bio-Rad, Hercules, CA, USA) with bovine serum albumin (Sigma-Aldrich Corporation, St. Louis, MO, USA) as standard. Proteins were diluted at a 1:1 ratio in loading buffer (10% sodium dodecyl sulphate (SDS), 2% glycerol, 5% bromophenol blue, 2-mercaptoethanol, and 0.5 M Tris-HCl; pH 6.8). The mixture samples were boiled for 5 min before the samples were subjected to 10% SDS-polyacrylamide gel electrophoresis (SDS-PAGE) at room temperature and 110 V for 90 min and electrotransferred to polyvinylidene fluoride (PVDF) membranes (Pall Corporation, Coral Gables, FL, USA) at a constant current of 30 V and at 4 °C overnight. Afterward, the PVDF membranes were washed twice in phosphate-buffered saline (PBS) containing 0.1% Tween 20 (PBS-T) for 10 min at room temperature. This process was performed three times. Then, we blocked the membranes surface with 5% non-fat dry milk in PBS at 37 °C for 1 h and saturated three times with PBS-T for 10 min at room temperature. Subsequently, the membranes were incubated in primary antibodies diluted at 1:1000 at 37 °C for 1 h. After three washes with PBS-T, the PVDF membranes were incubated with the horseradish peroxidase-conjugated secondary antibodies diluted at 1:10000 at 37 °C for 1 h to detect the bound primary antibody. The labeled proteins were visualized by enhanced chemiluminescence detection system (Amersham Biosciences, Amersham, UK), and the densities of the specific immunoreactive bands were quantified with a computer-assisted imaging densitometer system.

Co-immunoprecipitation

Here we describe protocols for protein-protein interaction assays that use protein G agarose to precipitate the target protein. Protein G agarose (Invitrogen, Carlsbad, CA) was washed in PBS and centrifuged for 2 min at 10,000 g. The supernatant was discarded, and the residue was subjected to two more washing cycles. Brain homogenates (1 mg) and p-PDGFR-β antibody were added to Protein G agarose and incubated at 4 °C overnight. Immune complexes were washed twice in dissociation buffer (0.5 M Tris-HCl, pH 8.0, 120 mM NaCl and 0.5% (v/v) Triton X-100). Next, the immune complexes were mixed with an equal volume of loading buffer (62.5 mM Tris-HCl, pH 6.8, 10% (v/v) glycerol, 2% (w/v) SDS, 5% (v/v) 2-mercaptoethanol, and 0.05% (w/v) bromophenol blue), heated at 95 °C for 5 min, and subjected to SDS-PAGE. The detection of target protein (p-PI3K) was determined by Western blotting.

Gelatin zymography

The procedures were based on zymography using SDS polyacrylamide gels containing gelatin as previously described.[14] Unboiled protein samples (30 μg) were added to an equal volume of standard loading buffer before loading. The samples were loaded on 7.5% (mass/volume) in polyacrylamide gels containing copolymerized substrate gelatin (0.1%) for SDS-PAGE (Sigma-Aldrich Corporation, St. Louis, MO, USA) to measure the gelatinase activities. SDS-

PAGE was performed in a running buffer (1% SDS, 25 mM Tris, and 250 mM glycine) at room temperature and 110 V for 1 h. After electrophoresis, each gel was washed twice for 30 min at each instance in the denaturing buffer (2.5% Triton X-100) at room temperature and washed twice with double-distilled water at room temperature for 10 min. The gel was then incubated in the reaction buffer (50 mM Tris-HCl, pH 7.5; containing 0.01% NaN_3, 0.02% Brij-35, and 10 mM $CaCl_2$) at 37 °C for 18 h, stained with 0.25% Coomassie Brilliant Blue R-250 (Bio-Rad, Hercules, CA, USA) for 1 h, and destained in a solution of 15% methanol/7.5% acetic acid. The final gel presented a uniform background, except in regions where gelatinases had migrated and cleaved their respective substrates. The gelatinases were quantitatively analyzed using a computer-assisted imaging densitometer system (UN-SCAN-ITTM gel Version 5.1, Silk Scientific, Provo, Utah, USA).

Double-staining immunofluorescence

Mouse brain tissues were fixed in 10% neutral buffer formalin. Several 5 μm-thick serial sections were cut from the brain of each mouse. For immunofluorescent labeling, non-specific binding was blocked with 3% BSA diluted in PBS-T. The brain sections were incubated at 4 °C overnight with the mixture of two primary antibodies (1:100 dilution), namely, those of PDGFR-β and MMP-9, to the SM α-actin monoclonal antibody. The mixture was decanted and washed three times with PBS for 5 min each in the dark. The sections were rinsed thrice with PBST and incubated with a mixture of two secondary antibodies, which were raised in different species (with two fluorochromes, i.e., Fluorescein AffiniPure Donkey Anti-Goat IgG and Cy™5 AffiniPure Donkey Anti-Goat IgG from Jackson ImmunoResearch Laboratories, West Grove, PA, USA) in 1% BSA for 1 h at room temperature in the dark. The sections were rinsed thrice with PBS, and mounted with a Vectashield mounting medium containing 4′,6- diamidino-2-phenylindole (DAPI) (Vector Laboratories, Burlingame CA, USA). The sections were mounted on a Zeiss LSM 510 META confocal microscope (Heidelberg, Germany).

ELISA

The production of S100B, interleukin (IL) −6 and transforming growth factor (TGF)-β in CSF was assayed using commercial ELISA kits (Abcan, USA) according to the manufacturer's instructions. CSF samples for cytokine assays were pooled since the amounts of CSF harvested from each mouse were often insufficient for individual assays.

BBB permeability evaluation

Evans Blue, a dye used to probe the integrity of the BBB, could enter the brain only during the pathological state. The steps have been adjusted in accordance with prior research findings.[15] The mice were injected with 2% (w/v) Evans Blue (5 mL/kg body weight; Sigma, St. Louis, MO, USA) in saline via the tail vein. After 2 h of circulation, the mice were anesthetized and transcardially perfused with saline to remove the intravascular dye. The brains were weighed and homogenized in 50% trichloroacetic acid solution. Brain tissue homogenates were centrifuged at 12,000×*g* for 10 min and the supernatants were collected. Each supernatant was measured at 620 nm for absorbance to calculate the concentration of Evans Blue using a spectrophotometer (Hitachi U3000, Tokyo, Japan).

Eosinophil counts in the CSF

The CSF was collected into a centrifuge for spinning at 400×*g* for 10 min. Sediments were gently mixed with 100 μL Unopette buffer (Vacutainer System, Becton Dickinson, Franklin Lakes, NJ, USA) and 2 μL acetic acid and used a hemocytometer cell counting chamber (Paul Marienfeld, Lauda-Koenigshofen, Germany) was used to count eosinophils.

Histology

The mouse brains were fixed with 10% neutral buffered formalin for 24 h. Fixed brains were dehydrated in a series of graded ethanol (50%, 75%, 95%, and 100%), replaced with xylene, and embedded in paraffin for 24 h. The serial sections were cut at 5 μm thickness of 5 m and stained with hematoxylin and eosin (Muto, Japan). Pathological changes were examined under a Zeiss light microscope.

Statistical analysis

Kruskal-Wallis nonparametric analysis followed by Dunn's multiple comparison tests was performed to evaluate differences among the different groups of mice. All outcomes were presented as means ± standard deviation (S.D.). Statistical significance was established for P values < 0.05.

Results

Influence of inhibitor-treated mice on signal proteins

The Western blot assay showed that the p-PDGFR-β, p-PI3K, and p-Akt in *A. cantonensis*-infected group were significantly higher than those in the control group. In the AG, LY and AG—LY groups, the levels of p-PDGFR-β, p-PI3K, and p-Akt were markedly lower ($P < 0.05$) than in the *A. cantonensis*-infected group (Fig. 1).

Interaction between p-PDGFR-β and p-PI3K

To investigate the interaction between p-PDGFR-β and p-PI3K, mouse brain samples were subjected to immunoprecipitation using targeted antibodies (anti-p-PDGFR-β and anti-p-PI3K). Analysis of the immunoprecipitates identified the presence of heavy chain and light chain. Two distinct experimental groups were examined: comprising uninfected mice and consisting of *A. cantonensis*-infected mice (Fig. 2).

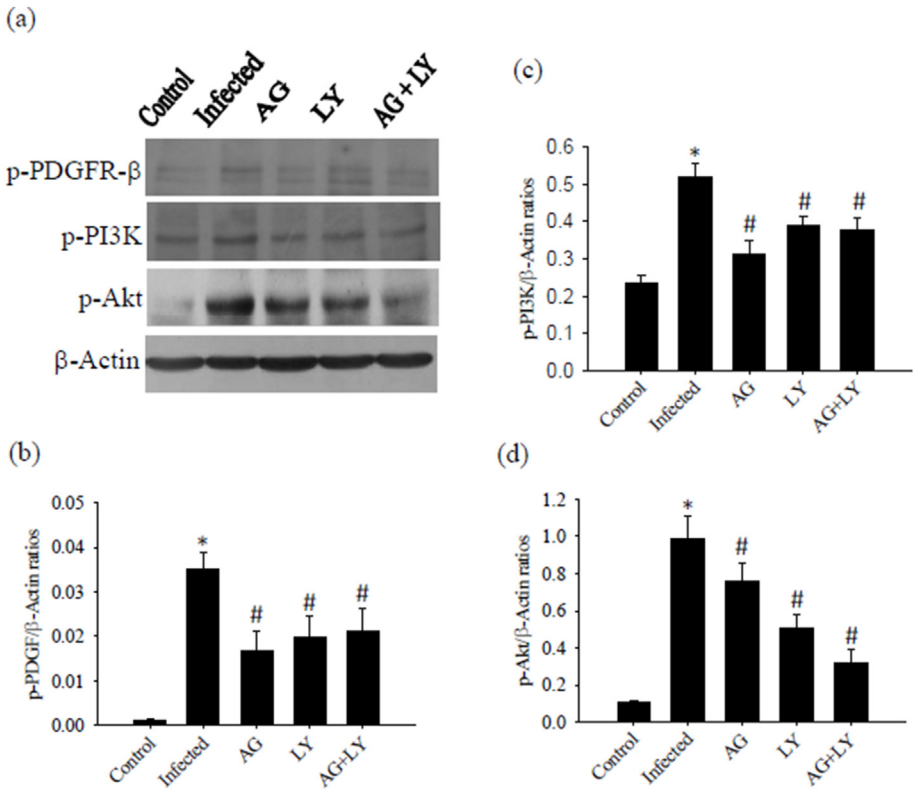

Figure 1. Changes of signal proteins. (a) Protein levels from mouse brains were analyzed by immunoblotting for platelet derived growth factor receptor-beta (PDGFR-β), phosphorylated phosphoinositide 3 kinase (p-PI3K), and phosphorylated protein kinase B (p-Akt). The infected mice were treated with AG1296 (AG), LY294002 (LY), or AG + LY co-treatment. β-Actin was used as a loading control. Quantification and normalization of PDGFR-β to β-actin (b), p-PI3K to β-actin (c), and p-Akt to β-actin (d) were performed with a computer-assisted imaging densitometer system. * indicates a statistically significant increase in *Angiostrongylus cantonensis*-infected mice compared with the control. # indicates a statistically significant decrease in the treated mice compared with *A. cantonensis*-infected mice.

Influence of inhibitor-treated mice on MMP-9 activity

Gelatin zymography measures showed that MMP-9 activity significantly increased ($P < 0.05$) in the brain of mice infected with *A. cantonensis*. The mice that received AG alone, LY alone, or AG—LY co-treatment showed significantly reduced ($P < 0.05$) MMP-9 activity (Fig. 3).

Localization of PDGFR-β in the smooth muscle cells of brain vessels

To confirm that PDGFR-β was localized in VSMCs, we performed co-immunofluorescence with the smooth muscle marker SM α-actin. The location of PDGFR-β in the smooth muscle cells of brain vessels was assessed using multiple staining techniques. DAPI staining (blue) highlighted nuclei, DyLight 488 staining (green) delineated smooth muscle cells, and rhodamine red staining (red) illustrated PDGFR-β distribution. The merged image demonstrated that PDGFR-β was colocalized with VSMCs (Fig. 4).

Localization of MMP-9 in the smooth muscle cells of brain vessels

Co-immunofluorescence microscopy was used to measure the co-localization of MMP-9 and SM α-actin in VSMCs. DAPI staining (blue) highlighted nuclei, DyLight 488 staining (green) delineated smooth muscle cells, and rhodamine red staining (red) illustrated MMP-9 distribution. The merged image conclusively demonstrated MMP-9 localization within the smooth muscle cells of brain vessels (Fig. 5).

Influence of inhibitor-treated mice and MMP-9 knockout mice on S100B, IL-6, and TGF-β

Sandwich ELISAs were used to assay S100B, IL-6, and TGF-β in the CSF to determine the kinetic production and their possible role in mouse resistance to *A. cantonensis*. The concentrations of S100B, IL-6, and TGF-β were significantly higher ($P < 0.05$) in the infected mice than in the uninfected ones. Compared with the infected—untreated mice, the S100B and IL-6 concentrations were significantly lower ($P < 0.05$) in the infected mice that received AG alone, LY

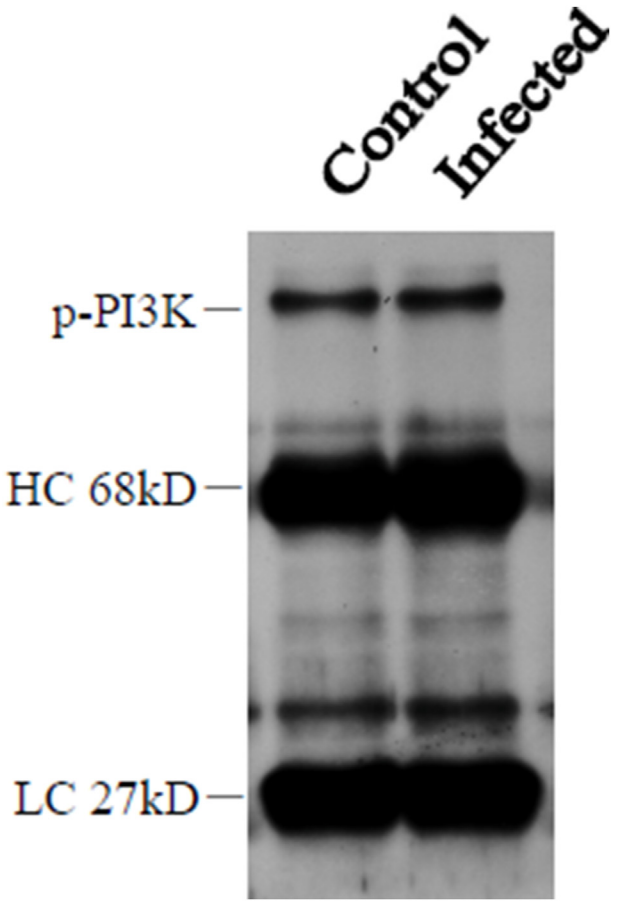

Figure 2. Interaction between phosphorylated platelet derived growth factor receptor-beta (p-PDGFR-β) and phosphorylated phosphoinositide 3 kinase (p-PI3K). Mouse brains were immunoprecipitated with the designated antibodies (anti-p-PDGFR-β and anti-p-PI3K) to determine the interaction between p-PDGFR-β and p-PI3K. HC: heavy chain; LC: light chain; Control: uninfected mice; Infected: *Angiostrongylus cantonensis*-infected mice.

alone, AG—LY co-treatment, or MMP-9 knockout mice. By contrast, the TGF-β concentrations were significantly higher ($P < 0.05$) in the infected mice that received AG alone, LY alone, AG—LY co-treatment, or MMP-9 knockout mice (Fig. 6).

Influence of inhibitor-treated mice and MMP-9 knockout mice on collagen type IV and fibronectin

The degraded protein levels of collagen type IV and fibronectin were significantly higher ($P < 0.05$) in the infected mice than in the uninfected mice. Compared to the outcomes for the infected—untreated mice, collagen type IV and fibronectin were significantly lowered ($P < 0.05$) in those who received AG alone, LY alone, AG—LY co-treatment, or MMP-9 knockout mice (Fig. 7).

Influence of inhibitor-treated mice and MMP-9 knockout mice on BBB permeability

The disruption of the BBB was estimated through Evans blue extravasation in the mouse model. Evans blue concentration is an indicator of BBB leakage during *A. cantonensis* infection in mice. The BBB permeability increased significantly in *A. cantonensis*-infected mice compared to that in the uninfected mice. Furthermore, BBB permeability was significantly attenuated in the mice treated with AG, LY, AG-LY co-treatment, or MMP-9 knockout mice (Fig. 8).

Influence of inhibitor-treated mice and MMP-9 knockout mice on eosinophil counts

The eosinophils were identified using the Unopette stained system. Eosinophil counts increased significantly in *A. cantonensis*-infected mice compared to uninfected mice. Eosinophils were significantly reduced in mice treated with AG, LY, AG-LY co-treatment, or MMP-9 knockout mice (Fig. 9).

Influence of inhibitor-treated mice and MMP-9 knockout mice on brain vasculature changes

H&E staining revealed immune cell aggregation around the brain vasculature of wild-type mice by day 20 PI with *A. cantonensis*. Conversely, this aggregation was subdued in mice treated with AG, LY, AG-LY co-treatment, or in MMP-9 knockout mice. Moreover, quantifying leukocytes in the cerebral vasculature via H&E-stained brain sections exhibited a significant decrease. These findings imply a correlation between the infiltration and aggregation of immune cells around brain vasculature and the involvement of PDGFR-β, PI3K, and MMP-9 during inflammation post-infection with *A. cantonensis* (Fig. 10).

Worm recovery

The effectiveness of AG alone, LY alone, AG—LY co-treatment, or MMP-9 knockout mice was assessed by recovering and counting viable larvae from brain tissues. The retrieval of *A. cantonensis* larvae was significantly higher ($P < 0.05$) in infected mice compared to uninfected ones. However, the larvae recovered from AG alone, LY alone, AG—LY co-treatment, or MMP-9 knockout mice exhibited a notable decrease ($P > 0.05$) compared to those from infected mice (Fig. 11).

Discussion

The neurovascular unit is a complex multi-cellular structure consisting of endothelial cells, neurons, glia, pericytes, VSMCs, and extracellular matrix (ECM).[16] Larger vessels are additionally enveloped by pericytes and VSMCs, which increase their stability and regulate their perfusion and form the BBB.[17] Vascular changes, including BBB destabilization, are common pathological features in angiostrongyliasis

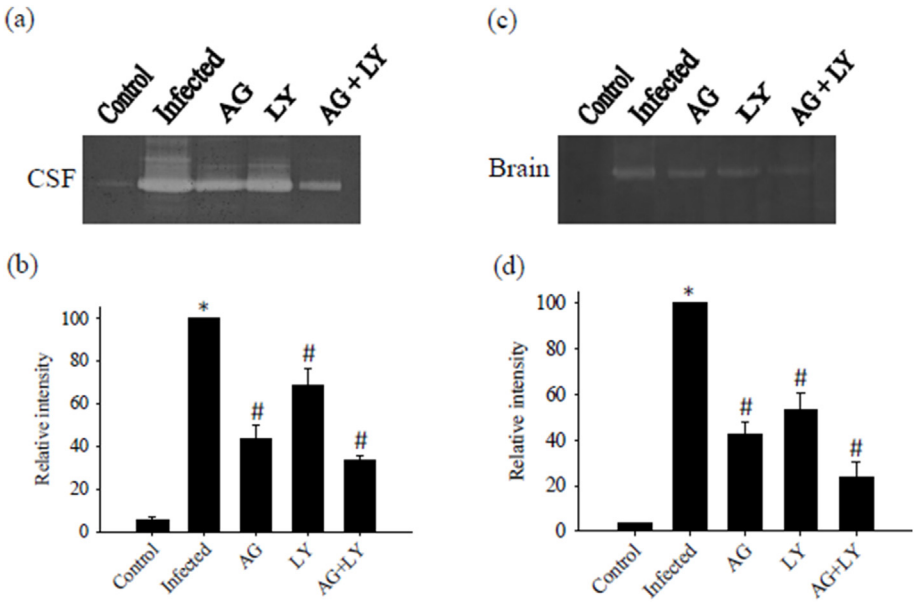

Figure 3. Changes of matrix metalloproteinase-9 (MMP-9). MMP-9 of cerebrospinal fluid (CSF) (a) or brain (c) were determined by zymography. The *Angiostrongylus cantonensis*-infected mice were treated with AG1296 (AG) alone, LY294002 (LY) alone, or AG + LY co-therapy. The relative intensities of the CSF (b) and brain (d) were quantified using a computer-assisted imaging densitometer system. *indicates a statistically significant increase in *A. cantonensis*-infected mice compared with the control. #indicates a statistically significant decrease in the treated-mice compared with *A. cantonensis*-infected mice.

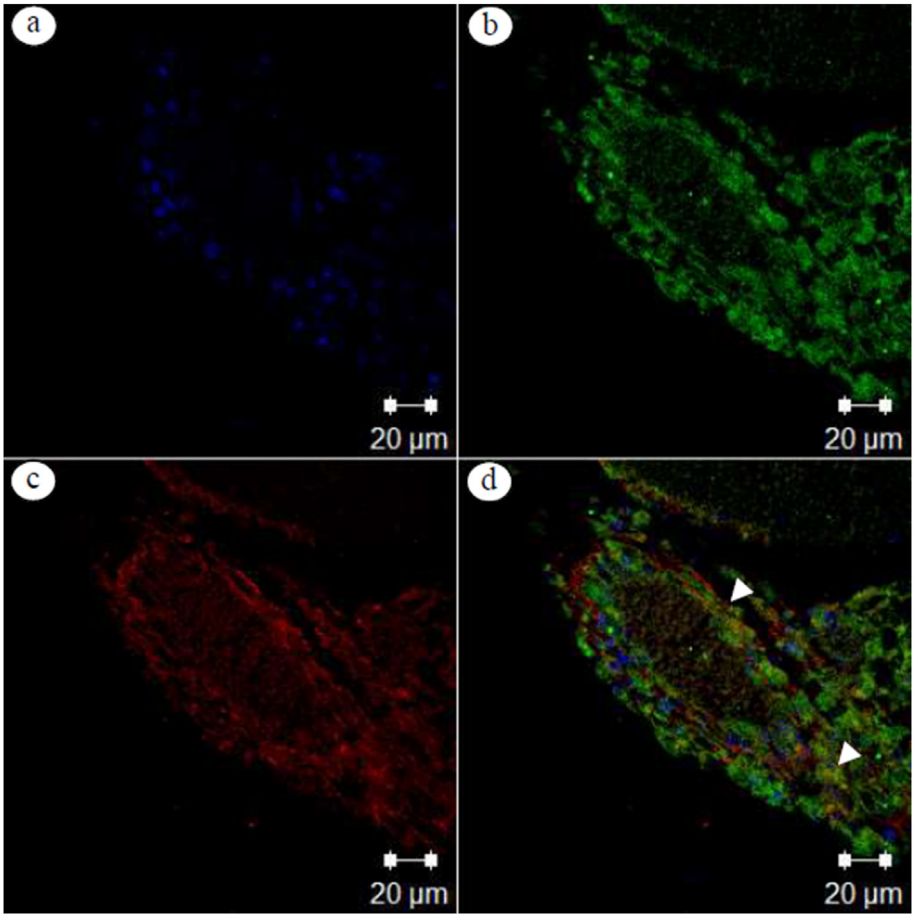

Figure 4. Localization of platelet derived growth factor receptor-beta (PDGFR-β) in the smooth muscle cells of brain vessels. (a) DAPI staining (blue) of nuclei; (b) DyLight 488 staining of smooth muscle cells (green); (c) rhodamine red staining of PDGFR-β (red); (d) merged image (yellow) showing that PDGFR-β was localized in the smooth muscle cells of brain vessels (white arrowheads).

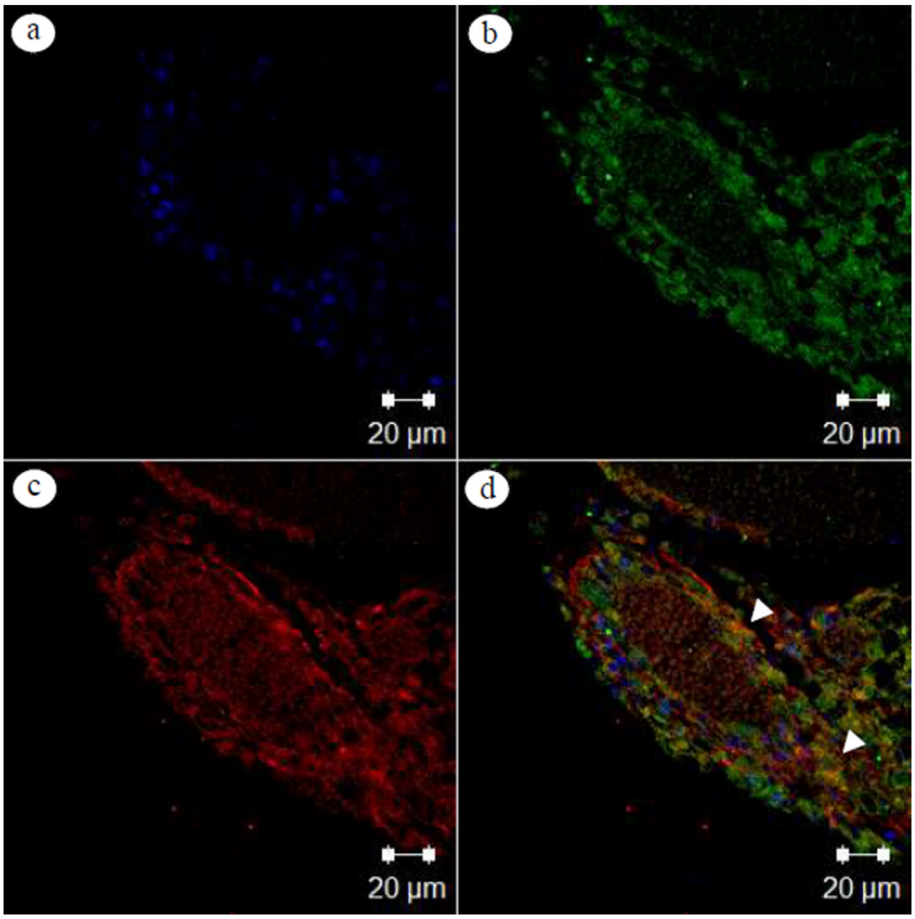

Figure 5. Localization of matrix metalloproteinase-9 (MMP-9) in the smooth muscle cells of brain vessels. (a) DAPI staining (blue) of nuclei; (b) DyLight 488 staining of smooth muscle cells (green); (c) rhodamine red staining of MMP-9 (red); (d) merged image (yellow) showing that MMP-9 was localized in the smooth muscle cells of brain vessels (white arrowheads).

meningoencephalitis.[18] BBB dysfunction is not always a binary "open or shut" phenomenon. Gradations in BBB permeability may reflect subtle perturbations in cell—cell signaling within the entire neurovascular unit.[19] VSMC modulation plays a key role in brain inflammation, whereby the contractile VSMCs are involved in migration. Another evidence shows that VSMCs may have a proinflammatory reaction and secrete MMP-9, which may functionally regulate infiltrated leukocytes during brain inflammation. Factors that drive the inflammatory reaction are not limited to cytokines but also include hemodynamic forces imposed on the blood vessel wall, intimate interaction of endothelial cells with VSMCs, and changes in the matrix composition of the vessel wall. This model is likely to be a useful tool for understanding the curative effects of AG1296 and LY294002 co-therapy in *A. cantonensis*-induced neurovascular unit dysfunction and can be valuable in the investigation of the influence of VSMCs on BBB in diseased states of angiostrongyliasis meningoencephalitis.

High levels of MMPs can damage the neurovascular matrix and cause BBB injury, edema, and hemorrhage.[20] Experimental models and clinical patient populations suggest that MMPs may disrupt BBB permeability and interfere with cell—cell signaling in the neurovascular unit.[21] Our previous study showed that MMP-9 can degrade BBB tight junction and function in the neurovascular unit, and it has been proposed as a potential biomarker in angiostrongyliasis meningoencephalitis.[3] However, very few research studied the matrix degradation of neurovascular unit in brain inflammation. In this study, MMP-9 knockout mice showed significant reductions in the two main components of the neurovascular matrix adhesion zone, that is, collagen type IV as the basement membrane component and fibronectin as a crucial part of the ECM. These results suggested that AG and LY co-therapy improved neurovascular matrix integrity and may comprise a set of mediators and targets for potential drug design to angiostrongyliasis meningoencephalitis.

VSMCs have been widely recognized as key players in the regulation of BBB function[22]; however, their mechanisms in angiostrongyliasis meningoencephalitis are unclear. This study aimed to identify the cell surface mechanoreceptors and intracellular signaling pathways that influence VSMCs to produce MMP-9 in response to *A. cantonensis* infection. Our approach was to evaluate the participation of the PDGFR-β/PI3K/Akt pathway in the expression of MMP-9 in mice with eosinophilic meningoencephalitis. For this purpose, MMP-9 activity was detected in *A. cantonensis*-infected mice in the presence of the PDGFR-β inhibitor AG. The results showed that MMP-9 activity was reduced by AG.

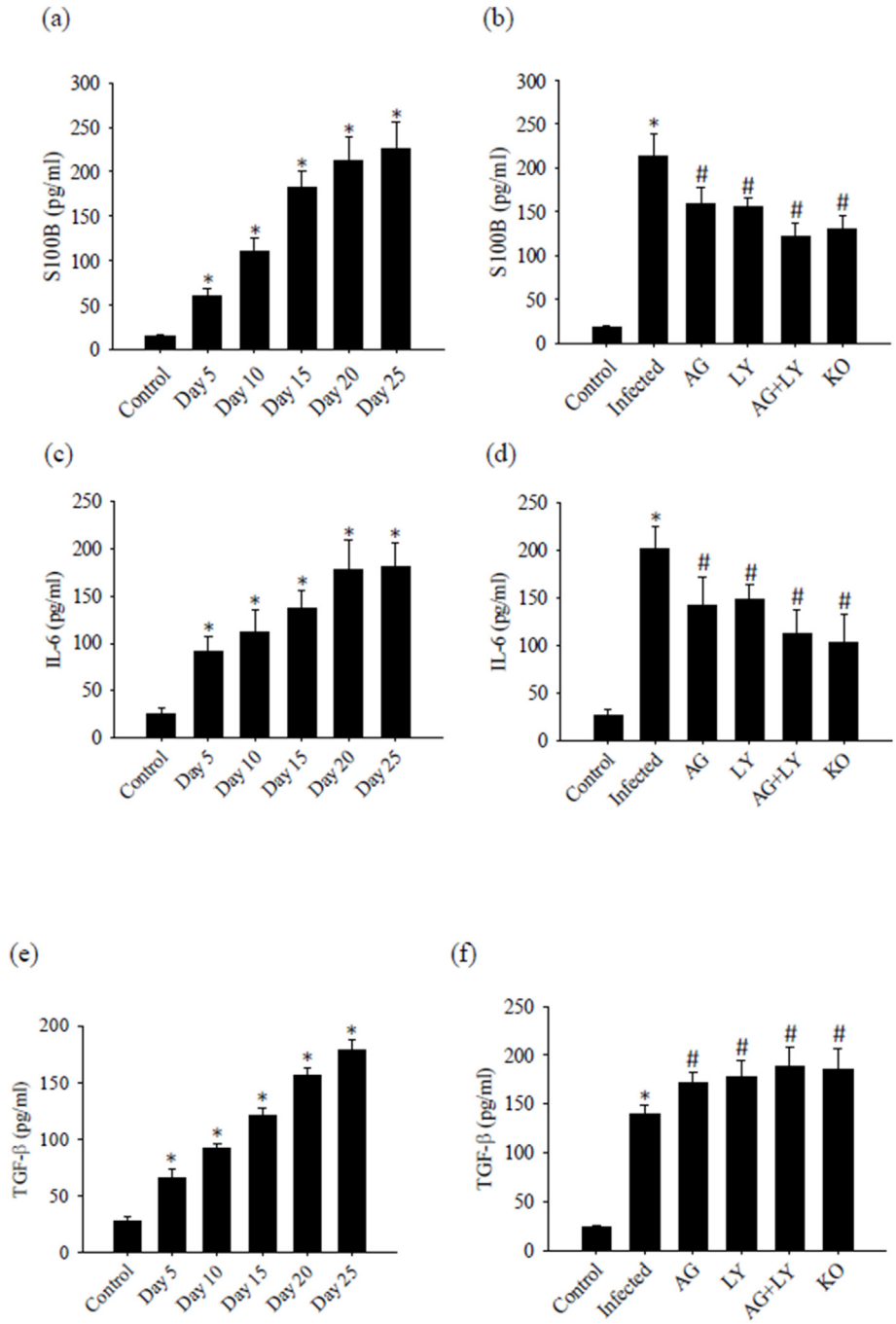

Figure 6. Changes in S100B and cytokines. Time-course studies of S100B (a), interleukin-6 (IL-6) (c), and transforming growth factor-beta (TGF-β) (e) in *Angiostrongylus cantonensis*-infected mouse brains were performed using ELISA. The concentrations of S100B (b), IL-6 (d), and TGF-β (f) were significantly different ($P < 0.05$) in *A. cantonensis*-infected mice compared with AG1296 (AG) alone, LY294002 (LY) alone, AG + LY co-therapy, or matrix metalloproteinase-9 (MMP-9) knockout (KO) mice. * indicates a statistically significant increase in *A. cantonensis*-infected mice compared with control. # indicates a statistically significant decrease in the treated mice and MMP-9 knockout mice compared with *A. cantonensis*-infected mice.

Furthermore, we explored whether PI3K/Akt signaling is involved in the expression of MMP-9. The mice that received PI3K inhibitor LY treatment also showed a significantly reduced MMP-9 activity. To further investigate the MMP-9 induced by PDGFR-β/PI3K/Akt signaling in VSMCs, we used co-immunoprecipitation assay and observed that PDGFR-β interacted with PI3K protein. Immunofluorescence showed that MMP-9 and the VSMC marker SM α-actin co-localized in the blood vessel. These data suggested that PDGFR-β inhibitor AG and PI3K inhibitor LY co-therapy blocked the activation of the PDGFR-β/PI3K/Akt signaling axis and reduced MMP-9 expression.

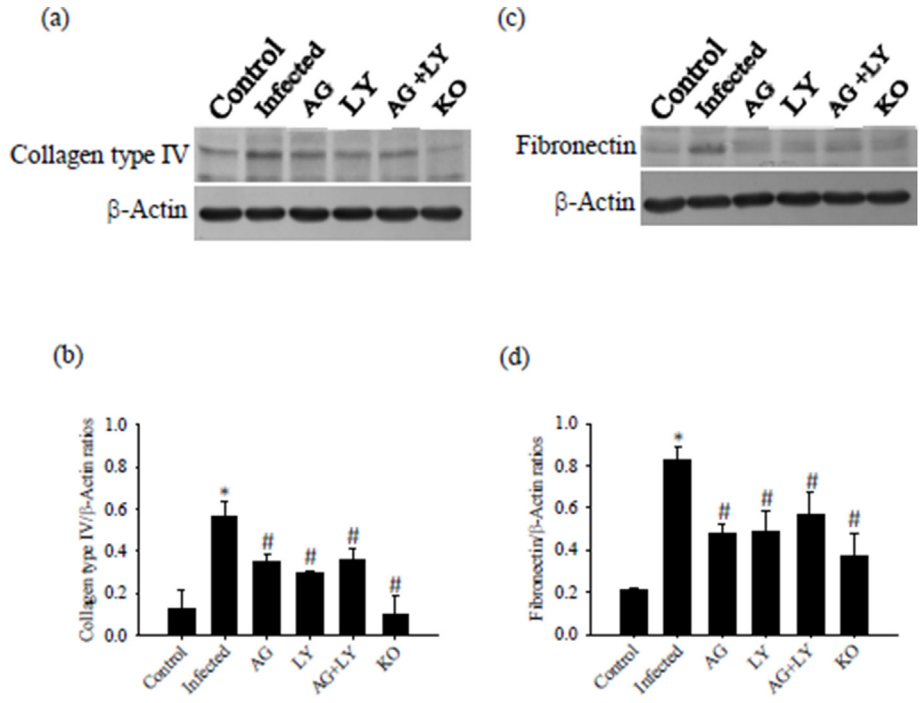

Figure 7. Degradation of collagen type IV and fibronectin. The degradation of collagen type IV (a) and fibronectin (c) was analyzed in the brains of wild-type, AG1296 (AG)-treated, LY294002 (LY)-treated, AG + LY co-treated, and matrix metalloproteinase-9 (MMP-9) knockout (KO) mice using Western blot analysis during *Angiostrongylus cantonensis* infection. Quantification and normalization of collagen type IV (b) and fibronectin (d) to β-actin were performed with a computer-assisted imaging densitometer system. *indicates a statistically significant increase in *A. cantonensis*-infected mice compared with the control. # indicates a statistically significant decrease in AG1296 (AG) alone, LY294002 (LY) alone, AG + LY co-therapy, or MMP-9 knockout (KO) mice compared with *A. cantonensis*-infected mice.

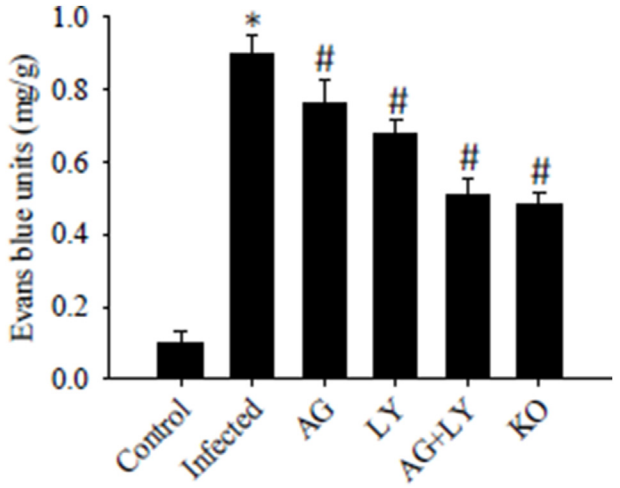

Figure 8. Changes of blood-brain barrier (BBB) permeability. Mouse BBB permeability was detected by extravasation of Evans Blue during *Angiostrongylus cantonensis* infection. Evans Blue dye units significantly increased (*$P < 0.05$) in *A. cantonensis*-infected mice (infected) compared with those in uninfected controls. Mice treated with AG1296 (AG) alone, LY294002 (LY) alone, AG + LY co-therapy, or MMP-9 knockout (KO) mice showed significantly lower (#$P < 0.05$) Evans Blue dye units compared with the untreated *A. cantonensis*-infected mice.

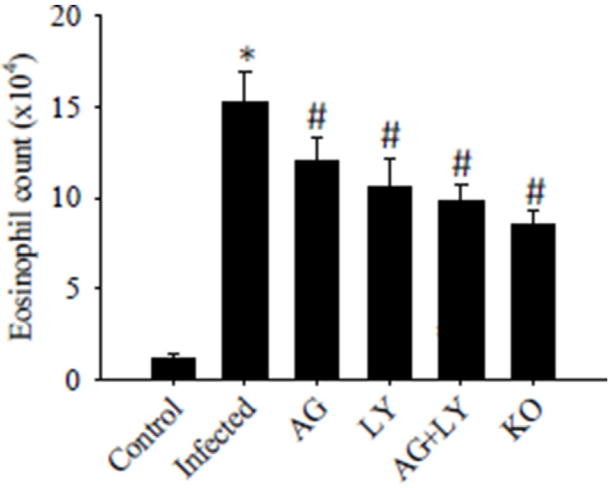

Figure 9. Changes of eosinophil counts. Eosinophil counts significantly increased (*$P < 0.05$) in *Angiostrongylus cantonensis*-infected mice compared with the uninfected controls. Treatment with AG1296 (AG) alone, LY294002 (LY) alone, AG + LY co-therapy, or matrix metalloproteinase-9 knockout (KO) mice significantly decreased (#$P < 0.05$) the eosinophil levels compared with the untreated infected mice.

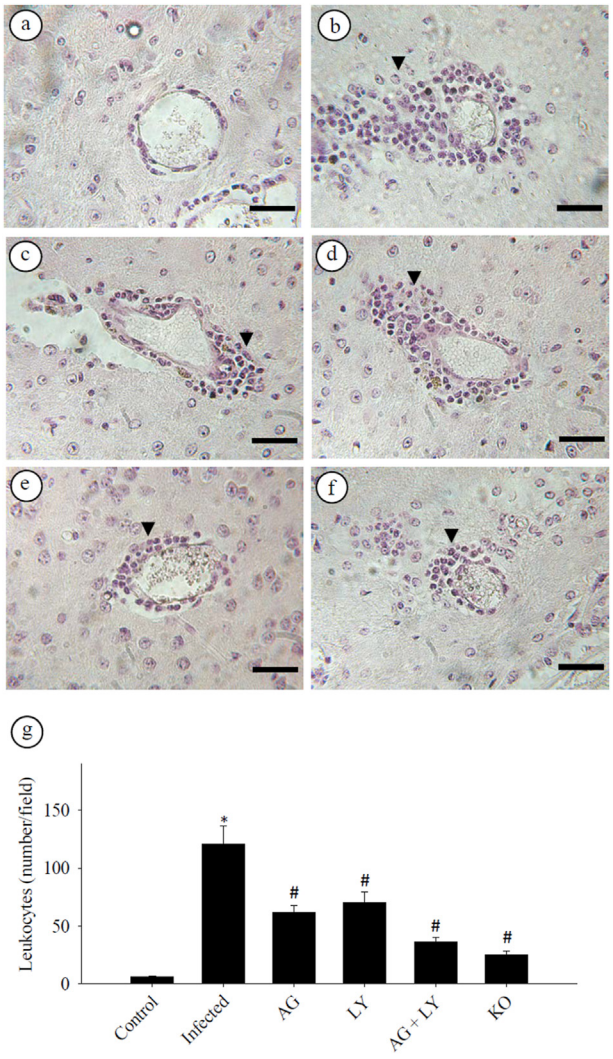

Figure 10. Histological results evaluated by H&E in brain vasculature. (a) Uninfected wild type mice. (b) Wild-type mice infected with *Angiostrongylus cantonensis* on day 20 post-inoculation. (c) Treatment with AG1296 (AG). (d) Treatment with LY294002 (LY). (e) Combined treatment with AG and LY. (f) Matrix metalloproteinase-9 knockout mice infected with *A. cantonensis* on day 20 PI. Arrowheads indicate infiltrated leukocytes. Bar scale = 80 μm. (g) Quantification of leukocytes in the brain vasculature using H&E stained brain sections.

Albendazole has been recognized for its efficacy against *A. cantonensis* owing to its larvicidal properties and its ability to mitigate the inflammatory response by reducing MMP-9 activity.[23] In this study, we assessed the effectiveness of AG alone, LY alone, AG—LY co-treatment, or MMP-9 knockout mice by recovering and quantifying viable larvae from brain tissues. It was observed that the retrieval of *A. cantonensis* larvae was notably higher in infected mice compared to uninfected ones. However, larvae recovered from mice treated with AG alone, LY alone, AG—LY co-treatment, or MMP-9 knockout showed a significant decrease compared to infected mice. Despite demonstrating

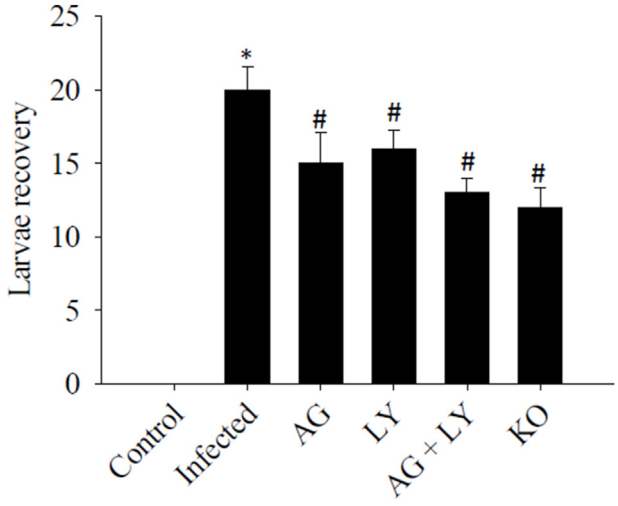

Figure 11. Worm recovery. The retrieval of *Angiostrongylus cantonensis* larvae exhibited a notable increase ($P < 0.05$) in infected mice compared to their uninfected counterparts. In contrast to the results observed in infected mice, the recovery of larvae markedly decreased ($P < 0.05$) in those administered AG alone, LY alone, AG—LY co-treatment, or in MMP-9 knockout mice.

statistically significant insecticidal effects, these treatments were found to be notably less effective than albendazole. Following treatment, the severity was substantially reduced, and symptoms did not recur. Additionally, neuroinflammation is regulated by the activities of endothelial, neuronal, and glial cells within the neurovascular unit, which serves as a platform for the coordinated action of pro- and anti-inflammatory mechanisms.[24] Specific biomarkers target neurovascular units, such as S100B and inflammatory cytokine IL-6.[25] Our previous study showed that S100B can be used as a biomarker in BBB damage in angiostrongyliasis meningoencephalitis.[18] In this study, we showed that AG and LY co-therapy significantly decreased S100B and pro-inflammatory cytokine IL-6 but significantly increased the anti-inflammatory cytokine TGF-β. This model may be a useful tool for future studies directed at understanding the pathogenesis of neurological inflammation associated with neurovascular unit dysfunction. These findings demonstrate that AG and LY co-therapy can reduce neuroinflammation in angiostrongyliasis meningoencephalitis.

Brain VSMCs are a critical component of the neurovascular unit and important in regulating BBB integrity.[11] We propose a possible mechanism (Fig. 12) to explain the contribution of PDGFR-β/PI3K/Akt signaling in VSMCs to BBB damage during *A. cantonensis* infection. AG inhibits PDGFRβ-induced PI3K/Akt in VSMCs during *A. cantonensis* infection, resulting in the reduction of MMP-9. In addition, AG treatment decreased matrix degradation and BBB permeability. The PI3K inhibitor LY had similar results. LY treatment decreased matrix degradation and BBB permeability. These results imply that AG and LY co-therapy inhibited the activation of the PDGFR-β/PI3K/Akt signaling axis and reduced neurovascular unit dysfunction.

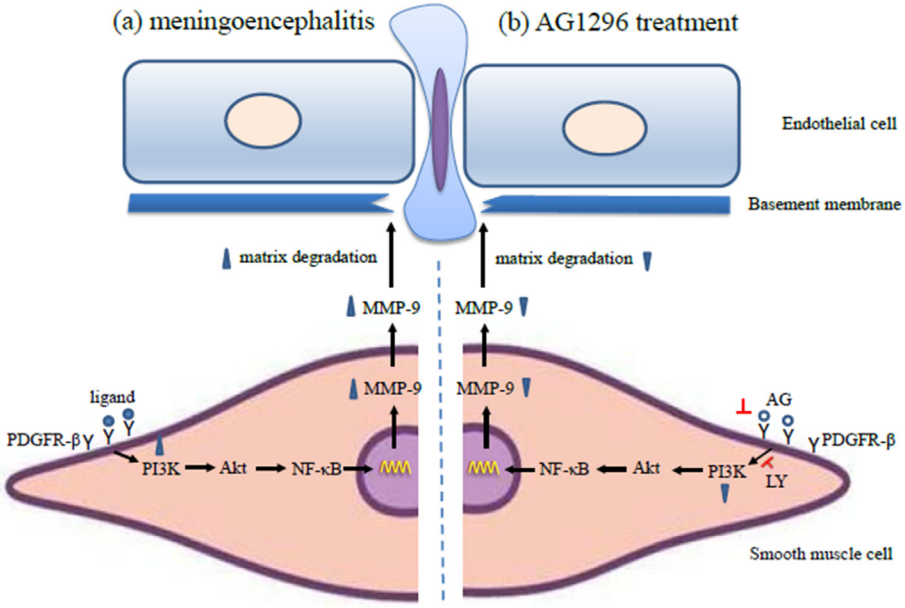

Figure 12. Possible mechanisms of AG1296 (AG) and LY294002 (LY) co-therapy in *Angiostrongylus cantonensis*-induced neurovascular unit dysfunction and eosinophilic meningoencephalitis. Vascular smooth muscle cell (VSMC) release MMP-9 which leading to neurovascular matrix integrity disruption via the platelet derived growth factor receptor-beta (PDGFR-β)/phosphorylated phosphoinositide 3 kinase (p-PI3K)/phosphorylated protein kinase B (p-Akt) signaling pathway. (a) Mice infected with *A. cantonensis* induced PDGFR-β/PI3K/Akt signaling proteins in the VSMC. The cell contributed to the elevation of MMP-9, which led to neurovascular matrix degradation. (b) Blocking of PDGFR-β signaling by AG can reduce PI3K/Akt signaling proteins, MMP-9 activity, and matrix protein degradation. Furthermore, LY inhibited PI3K/Akt signaling in VSMC during *A. cantonensis* infection, resulting in the reduced MMP-9 activity and matrix protein degradation.

The primary objective in designing and assessing drug combinations revolves around achieving synergistic effects, showcasing that the combined impact surpasses what would be expected from the sum of individual drug effects. Nevertheless, the co-administration of AG1296 and LY294002 fails to exhibit an additive effect on p-PDGFR-β and p-PI3K protein. This outcome may stem from two potential factors: (1) Interactions among biological signaling pathways create intricate networks due to their numerous components. (2) While drug combinations can yield synergistic effects, they may also produce antagonistic or additive outcomes. The amalgamation of therapies doesn't invariably ensure synergy or additivity and might involve risks of overlapping toxicity. Hence, there's an urgent need to comprehend the current status and underlying mechanisms of AG1296 and LY294002 combination therapy.

Our data indicated that *A. cantonensis* induced MMP-9 production in brain VSMCs through the activation of the PI3K/Akt pathway, which is mediated by activation of PDGFR-β signaling pathways. Inhibition of PDGFR-β signaling pathways preserved the integrity of the neurovascular matrix after experimental eosinophilic meningoencephalitis. Targeting PDGFR-β signaling may be advantageous in ameliorating brain inflammation following eosinophilic meningoencephalitis. Collectively, the brain infected with *A. cantonensis* induces MMP-9 production in VSMCs via the PDGFR-β-dependent activation of the PI3K/Akt pathway. These findings demonstrate the potential of PDGFR-β inhibitor AG and PI3K inhibitor LY co-therapy as anti-*A. cantonensis* drug candidates through improved neurovascular unit dysfunction and reduced inflammatory response.

Funding statement

This work was supported by grants from the Ministry of Science and Technology, R.O.C (MOST 109-2320-B-040-014-MY3).

CRediT authorship contribution statement

Ke-Min Chen: Data curation, Formal analysis, Investigation, Methodology, Software. **Shih-Chan Lai:** Conceptualization, Project administration, Supervision, Writing — original draft.

Declaration of competing interest

The authors declare no conflict of interest.

Acknowledgements

We wish to thank Ping-Sung Chiu of the Department of Parasitology, Chung Shan Medical University for providing invaluable assistance in the conduct of this study.

References

1. Mackerras MJ, Sandars DF. Lifehistory of the rat lung-worm and its migration through the brain of its host. *Nature* 1954;**173**:956—7.
2. Hsu WY, Chen JY, Chien CT, Chi CS, Han NT. Eosinophilic meningitis caused by *Angiostrongylus cantonensis*. *Pediatr Infect Dis J* 1990;**9**:443—5.
3. Chiu PS, Lai SC. Matrix metallopeinase-9 leads to claudin-5 degradation via the NF-κB pathway in BALB/c mice with eosinophilic meningoencephalitis caused by *Angiostrongylus cantonensis*. *PLoS One* 2013;**8**:e53370.
4. Grab DJ, Chakravorty SJ, van der Heyde H, Stins MF. How can microbial interactions with the blood-brain barrier modulate astroglial and neuronal function? *Cell Microbiol* 2011;**13**:1470—8. https://doi.org/10.1111/j.1462-5822.2011.01661.x.
5. Park JA, Choi KS, Kim SY, Kim KW. Coordinated interaction of the vascular and nervous systems: from molecule-to cell-based approaches. *Biochem Biophys Res Commun* 2003;**311**:247—53.
6. Newby AC. Matrix metalloproteinases regulate migration, proliferation, and death of vascular smooth muscle cells by degrading matrix and non-matrix substrates. *Cardiovasc Res* 2006;**69**:614—24.
7. Rubin K, Tingström A, Hansson GK, Larsson E, Rönnstrand L, Klareskog L, et al. Induction of B-type receptors for platelet-derived growth factor in vascular infammation: possible implications for development of vascular proliferative lesions. *Lancet* 1988;**1**:1353—6.
8. Zhan Y, Kim S, Izumi Y, Izumiya Y, Nakao T, Miyazaki H, et al. Role of JNK, p38, and ERK in platelet-derived growth factor-induced vascular proliferation, migration, and gene expression. *Arterioscler Thromb Vasc Biol* 2003;**23**:795—801.
9. Li SY, Johnson R, Smyth LC, Dragunow M. Platelet-derived growth factor signalling in neurovascular function and disease. *Int J Biochem Cell Biol* 2022;**145**:106187. https://doi.org/10.1016/j.biocel.2022.106187.
10. Seo KW, Lee SJ, Kim CE, Yun MR, Park HM, Yun JW, et al. Participation of 5-lipoxygenase-derived LTB(4) in 4-hydroxynonenal-enhanced MMP-2 production in vascular smooth muscle cells. *Atherosclerosis* 2010;**208**:56—61.
11. Potjewyd G, Kellett KAB, Hooper NM. 3D hydrogel models of the neurovascular unit to investigate blood-brain barrier dysfunction. *Neuronal Signal* 2021;**5**:NS20210027. https://doi.org/10.1042/NS20210027.
12. Parsons JC, Grieve RB. Effect of egg dosage and host genotype on liver trapping in murine larval toxocariasis. *J Parasitol* 1990;**76**:53—8.
13. Hou RF, Tu WC, Lee HH, Chen KM, Chou HL, Lai SC. Elevation of plasminogen activators in cerebrospinal fluid of mice with eosinophilic meningitis caused by *Angiostrongylus cantonensis*. *Int J Parasitol* 2004;**34**:1355—64.
14. Chen KM, Lee HH, Lu KH, Tseng YK, Hsu LS, Chou HL. Association of matrix metalloproteinase-9 and Purkinje cell degeneration in mouse cerebellum caused by *Angiostrongylus cantonensis*. *Int J Parasitol* 2004;**34**:1147—56.
15. Lok J, Zhao S, Leung W, Seo JH, Navaratna D, Wang X, et al. Neuregulin-1 effects on endothelial and blood-brain-barrier permeability after experimental injury. *Transl Stroke Res* 2012;**Suppl 1**(S1):S119—24. https://doi.org/10.1007/s12975-012-0157-x.
16. Zlokovic BV. Neurovascular pathways to neurodegeneration in Alzheimer's disease and other disorders. *Nat Rev Neurosci* 2011;**12**:723—38.
17. Kugler EC, Greenwood J, MacDonald RB. The "Neuro-Glial-Vascular" unit: the role of glia in neurovascular unit formation and dysfunction. *Front Cell Dev Biol* 2021;**9**:732820. https://doi.org/10.3389/fcell.2021.732820.
18. Chiu PS, Lai SC. Matrix metalloproteinase-9 leads to blood-brain barrier leakage in mice with eosinophilic meningoencephalitis caused by *Angiostrongylus cantonensis*. *Acta Trop* 2014;**140**:141—50. https://doi.org/10.1016/j.actatropica.2014.08.015.
19. Arvanitis CD, Ferraro GB, Jain RK. The blood-brain barrier and blood-tumour barrier in brain tumours and metastases. *Nat Rev Cancer* 2020;**20**:26—41. https://doi.org/10.1038/s41568-019-0205-x.
20. Cunningham LA, Wetzel M, Rosenberg GA. Multiple roles for MMPs and TIMPs in cerebral ischemia. *Glia* 2005;**50**:329—39.
21. Seo JH, Guo S, Lok J, Navaratna D, Whalen MJ, Kim KW, et al. Neurovascular matrix metalloproteinases and the blood-brain barrier. *Curr Pharmaceut Des* 2012;**18**:3645—8. https://doi.org/10.2174/138161212802002742.
22. Zhao Z, Nelson AR, Betsholtz C, Zlokovic BV. Establishment and dysfunction of the blood-brain barrier. *Cell* 2015;**163**:1064—78. https://doi.org/10.1016/j.cell.2015.10.067.
23. Lan KP, Wang CJ, Lai SC, Chen KM, Lee SS, Hsu JD, et al. The efficacy of therapy with albendazole in mice with parasitic meningitis caused by *Angiostrongylus cantonensis*. *Parasitol Res* 2004;**93**:311—7. https://doi.org/10.1007/s00436-004-1105-9.
24. Tohidpour A, Morgun AV, Boitsova EB, Malinovskaya NA, Martynova GP, Khilazheva ED, et al. Neuroinflammation and infection: molecular mechanisms associated with dysfunction of neurovascular unit. *Front Cell Infect Microbiol* 2017;**7**:276. https://doi.org/10.3389/fcimb.2017.00276.
25. Mir IN, Chalak LF. Serum biomarkers to evaluate the integrity of the neurovascular unit. *Early Hum Dev* 2014;**90**:707—11. https://doi.org/10.1016/j.earlhumdev.2014.06.010.